JBC Papers in Press. Published on November 11, 2008 as Manuscript M804860200
The latest version is at http://www.jbc.org/cgi/doi/10.1074/jbc.M804860200

DIFFERENTIAL INTERACTIONS OF THROMBOSPONDINS-1, -2 AND -4 WITH CD47 AND EFFECTS ON cGMP SIGNALING AND ISCHEMIC INJURY RESPONSES*

Jeff S. Isenberg[1, 4], Douglas S. Annis[2], Michael L. Pendrak[1], Malgorzata Ptaszynska[1], William A. Frazier[3], Deane F. Mosher[2], and David D. Roberts[1, 5]

From the Laboratory of Pathology[1], National Cancer Institute, National Institutes of Health, Bethesda, Maryland 20892; Departments of Biomolecular Chemistry and Medicine[2], University of Wisconsin, Madison, WI 53706; and Department of Biochemistry and Molecular Biophysics[3], Washington University School of Medicine, St. Louis, MO 63110

Running title: CD47 specificity for thrombospondins

[4]Current address: Hemostasis and Vascular Biology Research Institute and the Department of Medicine, University of Pittsburgh, Pittsburgh, PA 15260

[5]Address correspondence to: David D. Roberts, NIH, Building 10, Room 2A33, 10 Center Dr MSC1500, Bethesda, Maryland 20892 droberts@helix.nih.gov

Thrombospondin-1 regulates nitric oxide (NO) signaling in vascular cells via CD47. Because CD47-binding motifs are conserved in the C-terminal signature domains of all 5 thrombospondins, and indirect evidence has implied CD47 interactions with other family members, we compared activities of recombinant signature domains of thrombospondin-1, -2 and -4 to interact with CD47 and modulate cGMP signaling. Signature domains of thrombospondin-2 and -4 were less active than that of thrombospondin-1 for inhibiting binding of radiolabeled signature domain of thrombospondin-1 or SIRPα to cells expressing CD47. Consistent with this binding selectivity, the signature domain of thrombospondin-1 was more potent than those of thrombospondin-2 or -4 for inhibiting NO-stimulated cGMP synthesis in vascular smooth muscle cells and downstream effects on cell adhesion. In contrast to thrombospondin-1- and CD47-null cells, primary vascular cells from thrombospondin-2-null mice lack enhanced basal and NO-stimulated cGMP signaling. Effects of endogenous thrombospondin-2 on NO/cGMP signaling could be detected only in thrombospondin-1-null cells. Furthermore, tissue survival of ischemic injury and acute recovery of blood flow in thrombospondin-2-nulls resembles that of wild type mice. Therefore, thrombospondin-1 is the dominant regulator of NO/cGMP signaling via CD47, and its limiting role in acute ischemic injury responses is not shared by thrombospondin-2.

Nitric oxide (NO[1]) is a major mediator of intracellular and paracellular signal transduction. NO preserves vascular health by minimizing the adhesion of inflammatory cells to the vessel wall, limiting platelet activation, and increasing blood vessel diameter and blood flow by relaxing vascular smooth muscle cells (VSMC). These actions of NO are mediated by activating soluble isoforms of guanylate cyclase (sGC) to increase cGMP levels, resulting in downstream activation of cGMP-dependent protein kinases and ion channels (1).

Physiological NO/cGMP signaling is limited by several phosphodiesterases that degrade cGMP and by thrombospondin-1 (TSP). TSP1 is a secreted protein that is produced by vascular and inflammatory cells that regulates cellular behavior by engaging several cell surface receptors. Recently we reported that TSP1 potently blocks NO-stimulated prosurvival responses in endothelial and VSMC (2,3). TSP1 also plays a role in promoting platelet thrombus formation and hemostasis by antagonizing the antithrombotic activity of NO (4). In all of these vascular cells, picomolar concentrations of TSP1 are sufficient to block NO-stimulated fluxes in cGMP by engaging its receptor CD47 (5). Nanomolar concentrations of TSP1 further inhibit the same signaling pathway by inhibiting CD36-mediated uptake of myristate into vascular cells (6). In vivo, mice lacking TSP1 demonstrate elevated basal tissue cGMP levels and greater increases in regional blood flow in response to a NO challenge than wild type controls (4). Following an ischemic insult, the absence of TSP1 or CD47 in transgenic mice is associated with better maintenance of

tissue perfusion and enhanced tissue survival. Similarly, targeting TSP1 or CD47 using function blocking antibodies enhances ischemic tissue perfusion and survival in wild type mice and pigs (7,8).

TSP1 belongs to a family of five secreted glycoproteins that share an evolutionarily conserved C-terminal signature domain (9). TSP1 and TSP2 form a distinct subfamily of trimeric proteins that exhibit similar anti-angiogenic activities for endothelial cells in vitro and activities in vivo to block tumor growth. Despite their similarities in structure, TSP1 and TSP2 have markedly different expression patterns following tissue injury, with TSP1 being immediately expressed and maximal at day 3, whereas TSP2 was not expressed until day 7 and was maximal 10 days after injury (10). In addition, large amounts of TSP1 but not TSP2 are stored in platelet α-granules and released into the wound environment. Polymorphisms in TSP1 and TSP2 have been linked to altered risk of premature myocardial infarction (11,12). A 3' UTR polymorphism in TSP2 is also associated with type 2 diabetes in men (13). The molecular basis for these associations is unclear.

Less is known about the roles of the pentameric TSP3–5 in vascular cells. TSP3 and TSP5 (also known as cartilage oligomeric matrix protein) appear to serve their primary functions in bone development (14,15). However, a polymorphism in TSP4 is associated with premature myocardial infarcts in certain populations (11,16,17). A proatherogenic activity for the $A^{387}P$ variant of TSP4 was proposed based on its differential ability to modulate proliferation of endothelial and VSMC (18). Cardiovascular functions of TSP4 may also be linked to the high expression of TSP4 in heart (19) and its altered expression in that tissue during hypertensive heart failure (20).

The C-terminal domain of TSP1 is sufficient to mediate CD47-dependent inhibition of cGMP signaling (5). Of the two CD47-binding VVM motifs identified in this domain of TSP1, the first is conserved among all 5 TSPs, suggesting that CD47 binding could be a universal attribute of this family (21). Based on structural evidence that the VVM motifs may not be accessible (22,23), however, conservation of VVM motifs may not be sufficient to predict CD47 binding. Uncertainty regarding the location of the CD47 binding site in the G domain of TSP1, therefore, limits interpretation of the known sequence homology to predict CD47 binding to other TSP family members.

Although CD47 recognition of other TSPs has not been demonstrated experimentally, a local deficiency of inflammation-associated T cell apoptosis shared by TSP1, CD47, and TSP2 null mice is consistent with this hypothesis (24). Furthermore, a 21 residue peptide from the C-terminal domain of TSP4 was found to decrease human umbilical vein endothelial cell proliferation similar to the CD47 binding peptides from TSP1, although it lacks the VVM motif and no interaction with CD47 was demonstrated (25).

To directly address whether other TSP family members can inhibit NO-responses and signaling in vascular cells, we now compare binding of recombinant signature domains of TSP1, TSP2 and TSP4 to cell surface CD47 and inhibition of NO-stimulated cell responses and cGMP signaling by these domains. We also compared acute tissue blood flow and perfusion responses to ischemic challenge in TSP1 and TSP2 null mice and cGMP responses in primary cultures of vascular cells isolated from these mice. These studies clearly demonstrate that CD47 selectively interacts with TSP1 and that the signature domains of TSP2 and TSP4 are less potent inhibitors of NO signaling in vascular cells in vitro. Furthermore, we show that the role of TSP1 to acutely limit recovery from ischemic injury in vivo is not shared by TSP2.

EXPERIMENTAL PROCEDURES

Cells and reagents. Human aortic VSMC were obtained from Lonza (Switzerland) and maintained in the appropriate growth medium provided by the manufacturer. Wild type and CD47 negative (clone JinB8) Jurkat cells were obtained from Drs. Kevin Gardner and Eric Brown, respectively, and maintained in RPMI 1640 containing 10% FCS. The nitric oxide donors diethylamine/NONOate (DEA/NO) and diethylenetriamine/NONOate (DETA/NO) were provided kindly by Dr. Larry Keefer (NCI, Frederick, Maryland). Type I collagen was obtained from Inamed Biomaterials (Fremont, CA). TSP1 was prepared as previously described

from fresh platelets obtained under an approved protocol from the transfusion service of the National Institutes of Health (26). Recombinant proteins derived from TSP4 were expressed in insect cells using baculovirus (27). Recombinant regions of TSP1 and TSP2 as summarized in Fig. 1A were prepared as described (28). Recombinant extracellular domain of human SIRPα including all 3 Ig domains fused to a modified human Fc domain was prepared as described (29). SIRPα and E123CaG1 were labeled using $Na^{125}I$ by the Iodogen method as previously described for TSP1 (30). A CD47 monoclonal antibody (B6H12) was purified from conditioned medium of the corresponding hybridoma (American Type Culture Collection). An isotype-matched control IgG1 was obtained from Santa Cruz Biotechnology. TSP1 antibody A6.1 was obtained from Thermo Scientific (Cheshire, UK). An antisense morpholino oligonucleotide complementary to murine TSP2 mRNA (5'GGCCAGTGCCCAGAGCATCTTGTCT3') and a 5 base mismatched control morpholino were obtained from Gene Tools (Philomath, OR).

Animals. C57BL/6 wild type and TSP1 null mice were housed in a pathogen free environment with ad libatum access to water and rat chow on a 12 hour light-dark cycle. TSP2 null male mice 12 weeks of age and matched wild type mice in a B6129sf1/J background were obtained from Jackson Labs (Bar Harbor, ME). All animal studies conformed to the guidelines of the Animal Care and Use Committee of the National Cancer Institute of the NIH.

Primary murine vascular cell isolation. Using sterile technique, whole lungs were excised from 12 week old wild type, TSP1 and TSP2 null male mice and minced into 1–2 mm fragments and incubated in basal medium with collagenase type II (Worthington, MA). The cell suspension was then plated in standard culture flasks (Nunc, Denmark) in the presence of endothelial cell growth medium (Lonza) and used at the first passage. Under such conditions staining for CD31 has demonstrated 85-95% of cells to be endothelial cells (2).

Cell adhesion assay. Human aortic VSMC were plated at 10,000 cells/well onto 96-well plates (Nunc Maxisorb) precoated with type I collagen (3 μg/ml). Cells were incubated for 1 h in basal medium with 0.1% BSA and no growth factors and the indicated concentrations of recombinant TSP2, -3 and -4 domains ± DEA/NO. Plates were then washed with PBS, fixed with glutaraldehyde and stained with crystal violet, and washed. Absorbed stain was solubilized with acetic acid from fixed cells and quantified using a Micro580 Elisa plate reader (Dynatech Laboratories, Alexandria, VA) at 450 nm.

Cell proliferation assay. Primary wild type and TSP2 null lung derived endothelial cells were harvested as described (2) and plated at a density of 10,000 cells/well in standard endothelial cell growth medium ± NO (10 μM DETA/NO) and incubated for 72 hr at 37° C and 5% CO_2. 3-(4,5-dimethylthiazol-2-yl)-5-(3-carboxymethoxyphenyl)-2-(4-sulfophenyl)-2H-tetrazolium, inner salt (MTS) reagent (Promega, Madison, WI) was then added and the product quantified at 450 nm.

Intracellular cyclic GMP measurement. Yucatan white hairless pig femoral artery VSMC (8) or wild type, TSP1 and TSP2 null murine endothelial cells (10^5 cells/well) grown overnight in 6-well or 12-well culture plates (Nunc, Denmark) were pretreated for 24 h with medium containing 2% FCS and weaned off serum over 48 h before treatment with DEA/NO ± the indicated treatment agents in serum free medium containing 0.1% BSA. Intracellular cGMP levels were determined using an enzyme immunoassay (Amersham Biosciences, GE Healthcare) as per the manufacturer's instructions.

Hindlimb ischemia model. Wild type and TSP2 null 12 week old male mice underwent inhalation general anesthesia with 1.5% isoflurane. Using sterile techniques the femoral artery at the level of the inguinal ligament was identified and under operative magnification ligated with a 5-0 nylon suture and the skin incision closed. Limb perfusion was then measured at 5 minute intervals for the first hour postoperatively and at 72 h post-operatively via laser Doppler (Moor Instruments, Devon England). Also at 72 h post-operatively, vascular remodeling was assessed in the medial thigh musculature above and below the point of femoral artery ligation.

Laser Doppler Analysis. Dorsal cutaneous flap or hindlimb perfusion was determined in wild type and TSP2 null male mice under light general anesthesia via inhalation of 1.5% isoflurane. Core

body temperature was constantly monitored and maintained at 35°C. Pre-operative and post-operative perfusion flux levels were obtained at 5 min intervals with the following machine parameters: scan area – 1.6 x 2.5 cm; scan speed – 4 ms/pixel, scan time 1 min 54 sec, override distance 25 cm. The override distance was 20 cm. In hind limb studies the opposite unoperated limb served as an internal control.

Ischemic soft tissue flap model. Under inhalation isoflurane (1.5%), animals underwent creation of a random myocutaneous (McFarlane) flap as previously described (4). Flap viability was assessed 72 h post-operatively.

Determination of flap survival. Clinical assessment of flap perfusion was performed with notation of color, capillary refill and bleeding to needle stick being recorded. Flap dimensions were then traced onto a clear plastic sheet and with demarcation of viable and non-viable areas made. Weights of segments of sheeting corresponding to viable versus non-viable portions of flaps were then determined and % survival expressed as a percentage versus total as previously described (4).

CD47 binding studies. Jurkat T lymphoma cells ($1x10^6$ cells/well) were suspended in PBS containing divalent cations and 0.1% BSA with the indicated treatment reagents for 30 min. at 37°C. ^{125}I-SIRPα or ^{125}I-E123CaG1 was then added, and the cells were incubated at room temperature on a plate shaker for 1 h. Cells were separated by centrifugation through silicone oil (Nye Co, New Bedford, MA), and cell bound radioactivity was quantified using a Perkin Elmer gamma counter. Background counts in the absence of cells were determined for each experiment and subtracted to determine net binding.

Detection of TSP2 secretion. A heparin-BSA capture ELISA was used to detect TSP2 levels in the conditioned media. A 50 µL volume of heparin-BSA conjugate diluted to 100 ng/ml was adsorbed onto 96-well plate wells overnight at 4°C. The next day, the wells were blocked with 250 µL/well of 5 mM Tris , 1% BSA, 0.02mM phenylmethylsulfonyl fluoride, 150 mM NaCl, 1 mM $CaCl_2$, pH 7.8 for 30 min. Samples were dispensed at 50 µL per well and allowed to bind to the immobilized heparin-BSA for 2 h at 37°C. The wells were aspirated, and 50 µL of polyclonal anti-mouse TSP2 diluted 1:1000 in 50 mM Tris and 1% BSA was added to each well. The antibody was allowed to bind to the immobilized TSP2 for 2 h at 37°C. After aspiration, the wells were washed three times with 50 µL per well of Dulbecco's phosphate buffered saline (DPBS) with 0.02% BSA, .02 mM phenylmethylsulfonyl fluoride, and .05% Tween 20. Peroxidase conjugated goat anti-rabbit IgG (Kirkegaard and Perry) was diluted to 1:1000 in DPBS with 0.05% Tween-20 and allowed to bind for 1 h at room temperature. The wells were washed three times with DPBS with 0.05% Tween-20. A 50 µL volume of o-phenylenediamine dihydrochloride dissolved in phosphate-citrate buffer with sodium perborate (Sigma #P4922) and 30 µL hydrogen peroxide added just before use was added to each well. After 10 min, 3M sulfuric acid was added to stop the color development. Absorbance values were read at 490 nm.

Statistics. Results of vascular cell in vitro data are presented as the mean ± SD of at least three experiments. Significance was calculated with Student's t test or where appropriate one way and two way ANOVA using a standard software package (Origin) with $p < 0.05$. In vivo tissue survival and perfusion study results represent the mean ± SD of 5 pairs of wild type and TSP2-null animals.

RESULTS

Selective binding of the signature domain of TSP1 to CD47-expressing cells. Because others have failed to detect TSP1 binding to a recombinant extracellular domain of CD47 (22), we chose to examine TSP1 binding to native CD47 using a cell binding assay. TSP1 engages multiple cell surface receptors, and high affinity binding via the N domain to heparan sulfate proteoglycans is typically dominant in such cell binding studies (31). To detect CD47 binding, therefore, we used a recombinant signature domain of TSP1 that is known to mediate CD47-dependent signaling but lacks the high affinity heparin-binding site (Fig. 1A). The only other cell surface receptors known to interact with this domain are $\alpha_v\beta_3$ integrin, which is not expressed in Jurkat T lymphoma cells (32), and β_1 integrins, which interact with low affinity with the E123 domain (33). In Jurkat cells, β_1 integrin interaction with this domain of TSP1 requires activating signals that were not

present in these studies. Jurkat cells were also chosen for the binding studies based on their well characterized CD47-mediated responses to TSP1 (32) and the availability of a somatic mutant of the Jurkat line lacking CD47 (JinB8) (24).

^{125}I-labeled E123CaG1 bound at much higher levels to wild type Jurkat cells than to CD47-negative JinB8 cells (Fig. 1B). Furthermore, binding to Jurkat cells expressing CD47 was inhibited to background levels in a dose dependent manner by the function-blocking CD47 antibody B6H12 (Fig. 1C). An isotype matched control IgG_1 did not significantly inhibit binding of E123CaG1 at the same concentrations. Binding was also significantly inhibited by the TSP1-derived CD47-binding peptide ^{1102}FIRVVMYEGKK^{1112} (7N3) at 1 μM ($p = 0.02$) but not by the respective control peptide FIRGGMYEGKK (604, Fig. 1D).

Specific binding of ^{125}I-E123CaG1 to Jurkat cells was inhibited in the presence of 22 pM TSP1 (Fig. 1B), consistent with the known potency of TSP1 for inhibiting NO/cGMP signaling via CD47 (5). Unlabeled E123CaG1 was similarly active for self-inhibition of labeled ligand binding to Jurkat cells (Fig. 1E). In contrast, the corresponding signature domain of TSP2 (E123CaG2) was inactive over the same concentration range, and although the signature domain of TSP4 (E1234CaG4) produced consistent inhibition, the changes did not achieve significance (Fig. 1E). Therefore, high affinity interaction with CD47 appears to be relatively specific for the signature domain of TSP1.

Selective inhibition by TSP1 of SIRPα binding to cell surface CD47. We were concerned that the relatively high non-displaceable fraction of E123CaG1 binding in Fig. 1 could reflect residual interactions with other TSP1 receptors. Therefore, competition with the well characterized CD47 ligand SIRPα (34) was used to further assess TSP1 binding to cell surface CD47. TSP1 potently and dose-dependently inhibited ^{125}I-SIRPα binding to Jurkat cells (Fig. 2A). Analysis of the binding data using Scafit (version 2.4 of Ligand software (35)) gave an apparent dissociation constant for TSP1 of 12 pM with B_{max} of ~5000 sites/cell (Fig. 2A inset). The latter value is consistent with the known copy numbers for CD47 on other cell lines (36). The apparent K_d is consistent with the known potency of TSP1 for inhibiting cGMP signaling, but we caution that this number is dependent on assumptions used in the analysis and does not represent an intrinsic dissociation constant.

The requirement of CD47 for this interaction was confirmed by complete inhibition of ^{125}I-SIRPα binding to Jurkat cells in the presence of the CD47 blocking antibody B6H12 and the absence of ^{125}I-SIRPα binding to CD47-negative JinB8 cells (Fig. 2B). The dose dependence for B6H12 inhibition of SIRPα binding paralleled that for inhibiting E123CaG1 binding (compare Figs. 2C and 1C), and an isotype matched control IgG_1 did not significantly inhibit binding of SIRPα to wild type Jurkat cells (Fig. 2C).

E123CaG1 showed a similar dose-dependence for inhibiting SIRPα binding to Jurkat cells as intact TSP1, but the corresponding signature domains of TSP2 (E123CaG2) and TSP4 (E1234CaG4) were essentially inactive (Fig. 2D). This confirmed the relative specificity of CD47 for TSP1 and also established that TSP1 binding to CD47 can prevent interaction with its counter-receptor SIRPα. This has been hypothesized to occur in smooth muscle cells based on reduced co-immunoprecipitation of SIRPα with CD47 in the presence of TSP1 (37), but here is the first direct proof that such inhibition occurs at the level of SIRPα-CD47 binding.

Differential effects of TSPs on NO-driven cGMP in porcine VSMC. As previously reported for human VSMC (5), pretreatment of porcine VSMC with the full length signature domain of TSP1 (E123CaG1) before exposure to the rapidly releasing NO donor DEA/NO at 10 μM to activate sGC potently inhibited NO-stimulated cGMP accumulation in VSMC (Fig. 3A). The corresponding signature domains of TSP2 and TSP4 and a trimeric N-terminal region of TSP1 did not show significant inhibition under the same conditions (Fig. 3A). Decreasing the NO donor concentration to 1 μM, however, increased the sensitivity to inhibition by E123CaG1, and E123CaG2 and E1234CaG4 showed significant inhibition of cGMP levels under these conditions (Fig. 3B). The relative inhibitory potencies E123CaG1>E1234CaG4>E123CaG2 are consistent with their respective CD47 binding activities in Fig. 1E.

A truncated construct CaG1 retained inhibitory activity, showing that the EGF repeats of TSP1 are not required for activity (Fig. 3C). Consistent with the lesser activity of the full length TSP2 signature domain, CaG2 retained activity but was less active than CaG1. However, the isolated calcium wire (Ca1) only marginally changed cGMP levels, consistent with our previous report that bacterially expressed recombinant G1 is sufficient to inhibit NO-stimulated cGMP synthesis (5).

Because a polymorphism in the signature domain of TSP4 is associated with premature coronary artery disease (16), we also compared signature domains containing the normal sequence and the $A^{387}P$ variant for inhibiting cGMP signaling in porcine VSMC (Fig. 3D). No significant difference in inhibitory activity was noted for this variant, indicating that both variants can signal through CD47.

NO-stimulated VSMC adhesion on type I collagen is selectively blocked by the signature domain of TSP1. As previously reported (3), human aortic VSMC demonstrate enhanced adhesion to immobilized type I collagen in the presence of 10 μM DEA/NO, and the signature domain of TSP1 potently inhibits this stimulation (Fig. 4A). In the absence of NO, VSMC adhesion to collagen was not significantly altered by recombinant signature domains of either TSP1 or TSP2 (Fig. 4B). Similar to their effects on cGMP levels, signature domains of TSP2 and TSP4 did not significantly inhibit NO-stimulated adhesion at a concentration sufficient for the corresponding domain of TSP1 to maximally inhibit this response (Fig 4C, $p = 0.006$).

Endogenous TSP2 does not limit NO-driven cGMP flux in vascular cells. The absence of either TSP1 or its receptor CD47 was previously shown to elevate basal and NO-stimulated cGMP levels in primary murine vascular cells (2,5). To assess whether endogenous TSP2 can significantly limit NO/cGMP signaling in vascular cells, wild type and TSP2-null lung-derived murine endothelial cells were treated with exogenous NO and cGMP levels assayed (Fig. 5A). In untreated cells, no difference was seen between wild type and TSP2 null cell cGMP levels. Following NO treatment, cGMP levels were moderately but consistently lower in TSP2-null endothelial cells ($p<0.05$ in 3 independent experiments). NO/cGMP signaling also stimulates proliferation in these cells (2), but we observed no significant differences in basal or NO-stimulated proliferation between wild type and TSP2 null lung endothelial cells (Fig. 5B, $p = 0.38$).

Although both of these results suggest that endogenous TSP2 expressed by vascular cells does not limit their sGC response to NO, it is possible that these cells do not express sufficient concentrations of TSP2 to limit this response. Quantitative real time RT-PCR confirmed expression of TSP2 mRNA in primary cultures of wild type lung endothelial cells, but the level was somewhat lower than that of TSP1 mRNA (Fig. 5C). Therefore, the endogenous TSP1 produced by these cells may mask any activity of the endogenous TSP2.

To more clearly define the ability of endogenous TSP2 to modulate cGMP signaling, we used primary TSP1 null vascular cells and employed an antisense morpholino to suppress TSP2 expression. In wild type primary cells, pretreatment with the morpholino had no significant effect on basal or NO-stimulated cGMP levels (Fig. 5D). However, pre-treatment of primary TSP1 null endothelial cells with the TSP2 morpholino demonstrated increased intracellular cGMP after stimulation with exogenous NO compared to the response of cells treated with a 5 base mismatched control morpholino (Fig. 5D, $p = 0.02$ and 0.08 in 2 independent experiments). A heparin capture ELISA assay confirmed significant suppression of TSP2 secretion by the morpholino-treated cells that was lacking in cells treated with the mismatched control morpholino (Fig. 5E). Because we lack purified native TSP2 as a standard, it was not possible to quantify the extent of suppression. These data establish that, endogenous TSP2 can limit NO/cGMP signaling, but this activity is normally masked by the greater activity of endogenous TSP1.

Ischemic cutaneous tissue survival is not limited by TSP2. Although TSP2 only weakly limited cGMP signaling in lung endothelial cells in vitro, we wanted to determine whether endogenous TSP2 has any effect in vivo under ischemic stress conditions. We previously reported that endogenous TSP1 and CD47 limit ischemic tissue survival in dorsal random skin flaps in a C57BL/6 background (4,38). We found that wild type 129SvJ/BL6 are more resistant to the dorsal flap

injury than C57BL/6 mice but observed no difference between wild type and TSP2-null animals assessed 72 h post-operatively (Fig. 6A). Furthermore, the rate of acute decrease in flow in the ischemic flaps as assessed in the first 60 minutes following surgery using laser Doppler imaging did not differ between TSP2 null mice and their wild type controls (Fig. 6B). Therefore, endogenous TSP2 does not acutely limit tissue perfusion under these conditions.

Hindlimb perfusion under ischemic challenge is not limited by TSP2. Because mice in this background appear to be relatively resistant to skin flap ischemia, we turned to a more severe fixed ischemic injury model using femoral artery ligation of the hindlimb. A similar though not identical hindlimb model was recently shown to have moderately improved long term restoration of flow in the TSP2 null (39). Wild type and TSP2-null 12 week old male mice underwent ligation of the femoral artery. Laser Doppler analysis was then performed. During the first post-operative h, both wild type and TSP2-null animals demonstrated profound decreases in hindlimb perfusion (Fig. 7A). Analysis of hindlimb perfusion 72 h post-operatively demonstrated similar persistence in the perfusion defect in wild type and TSP2 null mice (Fig. 7B), and clinical assessment indicated no acute advantage of the TSP2 null mouse in this ischemic injury model.

DISCUSSION

The present results establish that the signature domain of TSP1 is a ligand for cell surface CD47 and demonstrate more avid recognition by cell surface CD47 of the signature domain of TSP1 versus those of TSP2 and TSP4. The signature domain of TSP1 binds with high affinity only to CD47-positive T cells, and its binding is inhibited by a known CD47 blocking antibody. This selectivity correlates with stronger inhibition of NO/cGMP signaling by the signature domain of TSP1 and suggests a more potent activity of TSP1 as opposed to TSP2 or TSP4 for blocking NO-stimulated vascular cell responses and tissue perfusion and survival under ischemic challenge. Despite the similar activities of TSP1 and TSP2 for inhibiting tumor growth and tumor-driven angiogenesis (40,41), TSP1 more potently inhibits NO/cGMP signaling in vascular cells. Indeed, significant effects of endogenous TSP2 on NO/cGMP signaling in vascular cells can only be detected in TSP1 null cells. We have previously shown that TSP1 inhibits NO/cGMP signaling via CD36, which is also a TSP2 receptor (42), but only at nanomolar concentrations (6). Therefore, the selective interaction of TSP1 with CD47 rather than CD36 is critical for its potent inhibition of NO/cGMP signaling.

The differential activities of recombinant signature domains of TSP1 and TSP2 for binding to CD47 are reflected in the phenotypes of TSP1 and TSP2 null mice. Vascular cells and platelets lacking TSP1 demonstrate significant differences in both basal and NO-stimulated cGMP levels compared to cells that produce functional TSP1 (2,3,43). In contrast vascular cells obtained from TSP2-null animals do not demonstrate differences in cGMP accumulation under either basal or NO-stimulated conditions.

Although initial studies clearly identified CD47 as a receptor for two synthetic peptides derived from the signature domain of TSP1 (21), some recent publications have raised concerns about the relevance of such peptide binding to physiological TSP1 signaling through CD47. Independent studies have concluded that some signaling responses to such peptides can be CD47-independent (44). Although genetic evidence has established that CD47 is necessary for a number of signaling responses to TSP1 (5,32,44), direct binding of native TSP1 to this receptor has not previously been reported. Furthermore, surface plasmon resonance studies using a recombinant extracellular domain of CD47 that was verified to bind to its other known ligand SIRPα failed to detect TSP1 binding (22). This could be interpreted as evidence that TSP1 does not directly bind to CD47, but the recombinant CD47 domain used may simply exist in a conformation that selectively precludes TSP1 binding. Recent computational modeling also suggests that CD47 binding may require a conformation change in TSP1 (45). Our current data show that saturable binding of the signature domain of TSP1 to the surface of Jurkat cells requires CD47 and is inhibited by a function-blocking CD47 antibody. Furthermore, binding of SIRPα to CD47 on the same cells is potently inhibited by TSP1. Therefore, it is clear that platelet TSP1 exists in a conformation that can bind to CD47 and does so

via its signature domain. We further established that the G module is required for this interaction.

The weaker activity of signature domains from TSP2 and TSP4 to compete with that of TSP1 for binding to CD47 or to inhibit SIRPα binding suggests that conservation of VVM motifs is not sufficient for high affinity binding of other TSPs to CD47. Notably, we found that the CD47-binding peptide 7N3 does compete with the signature domain of TSP1 for binding to cell surface CD47, and disrupting the VVM motif in the peptide abolishes this activity. Although computational modeling suggests that the VVM could become exposed in intact TSP1 (45), other residues in this active peptide are exposed in the published crystal structure and may play more important roles in CD47 binding. We propose that mutating the VVM motif in the peptide 7N3 changes the conformation of these adjacent residues to prevent its binding to CD47.

Defining the CD47 binding site in the signature domain of TSP1 still requires further study. One necessary step will be to solve the structure of native CD47. The existing recombinant domains of CD47 may not be suitable for this purpose based on their failure to replicate the binding of TSP1 to native CD47 on the cell surface (22). Interactions with the membrane spanning domain of CD47 may alter the conformation of the extracellular domain to permit TSP1 binding. Indeed a disulfide bond connects the IgV domain to a cell surface loop of the transmembrane domain of CD47 in its native structure (46). An additional possibility is that specific interactions of CD47 with other proteins on the cell surface such as integrins may be required to enable high affinity TSP1 binding.

In vivo, endogenous TSP1 continuously limits cGMP levels in vascular cells and thereby antagonizes NO to maintain blood pressure and platelet homeostasis. Consequently, TSP1-null animals demonstrate enhanced tissue perfusion and survival to various ischemic challenges compared to wild type animals due to enhanced NO/cGMP responses (4,38,43). In contrast, TSP2-null animals showed no tissue survival or perfusion advantage in the same ischemia models. TSP2 may play other roles in cardiovascular pathophysiology, but it does not play a major role in ischemic injury responses. Similarly, we recently showed that TSP2 null mice do not replicate the radioresistance phenotypes of TSP1- and CD47-null mice (47).

The weak activity of TSP2 to inhibit NO/cGMP signaling via CD47 may explain why TSP2-null animals respond so poorly to ischemic challenge. Strain-specific characteristics may account for some variation in responses to ischemia since the TSP1-null is in a C57Bl/6 background whereas the TSP2-null is in a B6129sf1/J background. Nonetheless, despite the reported overall increase in vascular density in the TSP2-null basally and following wounding (48), these animals consistently showed no acute advantage in tissue perfusion and survival in two fixed ischemia models compared to their respective controls and a modest long term advantage that was attributed to increased arteriogenesis and matrix remodeling in a third model employing hindlimb arteriectomy (39). In contrast, TSP1-null animals always show dramatic acute increases in tissue blood flow, perfusion and survival compared to controls in ischemic stress models (4,7,43,49).

The dominant activity of TSP1 in blocking NO-driven sGC activation is particularly important since it is by sGC activation through cGMP that NO stimulates dephosphorylation of myosin light chain 2 to relax VSMC. These findings underscore the priority role TSP1 plays in regulating NO-driven responses in vascular cells and ischemic tissues. We caution that our results to not preclude roles of TSP2 and TSP4 in modulating NO/cGMP signaling via CD47 in other disease states. In tissues that express high levels of these TSPs, their weaker interactions with CD47 may be sufficient to inhibit NO/cGMP signaling. For example, TSP4 is highly expressed in heart (19), so it may significantly engage CD47 in that tissue.

Acknowledgements
We thank Dr. Larry Keefer for providing the NO donors.

Footnotes

*This research was supported by the Intramural Research Program of the NCI, National Institutes of Health, Center for Cancer Research (DDR) and NIH grants HL54462 (DFM) and HL54390 (WAF).

[1]The abbreviations used are: DEA/NO, diethylamine NONOate; DETA/NO, diethylenetriamine/NONOate; NO, nitric oxide; sGC, soluble guanylate cyclase; SIRP, signal-regulatory protein; TSP, thrombospondin; VSMC, vascular smooth muscle cells

REFERENCES

1. Ignarro, L. J. (2002) *J Physiol Pharmacol* **53**, 503-514
2. Isenberg, J. S., Ridnour, L. A., Perruccio, E. M., Espey, M. G., Wink, D. A., and Roberts, D. D. (2005) *Proc Natl Acad Sci U S A* **102**, 13141-13146
3. Isenberg, J. S., Wink, D. A., and Roberts, D. D. (2006) *Cardiovasc Res* **71**, 785-793
4. Isenberg, J. S., Hyodo, F., Matsumoto, K., Romeo, M. J., Abu-Asab, M., Tsokos, M., Kuppusamy, P., Wink, D. A., Krishna, M. C., and Roberts, D. D. (2007) *Blood* **109**, 1945-1952
5. Isenberg, J. S., Ridnour, L. A., Dimitry, J., Frazier, W. A., Wink, D. A., and Roberts, D. D. (2006) *J Biol Chem* **281**, 26069-26080
6. Isenberg, J. S., Jia, Y., Fukuyama, J., Switzer, C. H., Wink, D. A., and Roberts, D. D. (2007) *J Biol Chem* **282**, 15404-15415
7. Isenberg, J. S., Romeo, M. J., Abu-Asab, M., Tsokos, M., Oldenborg, A., Pappan, L., Wink, D. A., Frazier, W. A., and Roberts, D. D. (2007) *Circ Res* **100**, 712-720
8. Isenberg, J. S., Romeo, M. J., Maxhimer, J. B., Smedley, J., Frazier, W. A., and Roberts, D. D. (2008) *Ann Surg* **247**, 860-868
9. Carlson, C. B., Lawler, J., and Mosher, D. F. (2008) *Cell Mol Life Sci* **65**, 672-686
10. Agah, A., Kyriakides, T. R., Lawler, J., and Bornstein, P. (2002) *Am J Pathol* **161**, 831-839
11. Topol, E. J., McCarthy, J., Gabriel, S., Moliterno, D. J., Rogers, W. J., Newby, L. K., Freedman, M., Metivier, J., Cannata, R., O'Donnell, C. J., Kottke-Marchant, K., Murugesan, G., Plow, E. F., Stenina, O., and Daley, G. Q. (2001) *Circulation* **104**, 2641-2644
12. Boekholdt, S. M., Trip, M. D., Peters, R. J., Engelen, M., Boer, J. M., Feskens, E. J., Zwinderman, A. H., Kastelein, J. J., and Reitsma, P. H. (2002) *Arterioscler Thromb Vasc Biol* **22**, e24-27
13. Yamaguchi, S., Yamada, Y., Matsuo, H., Segawa, T., Watanabe, S., Kato, K., Yokoi, K., Ichihara, S., Metoki, N., Yoshida, H., Satoh, K., and Nozawa, Y. (2007) *Int J Mol Med* **19**, 631-637
14. Hankenson, K. D., Hormuzdi, S. G., Meganck, J. A., and Bornstein, P. (2005) *Mol Cell Biol* **25**, 5599-5606
15. Posey, K. L., Hayes, E., Haynes, R., and Hecht, J. T. (2004) *Int J Biochem Cell Biol* **36**, 1005-1012
16. Wessel, J., Topol, E. J., Ji, M., Meyer, J., and McCarthy, J. J. (2004) *Am Heart J* **147**, 905-909
17. Cui, J., Randell, E., Renouf, J., Sun, G., Green, R., Han, F. Y., and Xie, Y. G. (2006) *Am Heart J* **152**, 543 e541-545
18. Stenina, O. I., Desai, S. Y., Krukovets, I., Kight, K., Janigro, D., Topol, E. J., and Plow, E. F. (2003) *Circulation* **108**, 1514-1519
19. Lawler, J., Duquette, M., Whittaker, C. A., Adams, J. C., McHenry, K., and DeSimone, D. W. (1993) *J Cell Biol* **120**, 1059-1067
20. Rysa, J., Leskinen, H., Ilves, M., and Ruskoaho, H. (2005) *Hypertension* **45**, 927-933
21. Gao, A. G., Lindberg, F. P., Finn, M. B., Blystone, S. D., Brown, E. J., and Frazier, W. A. (1996) *J Biol Chem* **271**, 21-24

22. Adams, J. C., Bentley, A. A., Kvansakul, M., Hatherley, D., and Hohenester, E. (2008) *J Cell Sci* **121**, 784-795
23. Kvansakul, M., Adams, J. C., and Hohenester, E. (2004) *Embo J* **23**, 1223-1233
24. Ticchioni, M., Raimondi, V., Lamy, L., Wijdenes, J., Lindberg, F. P., Brown, E. J., and Bernard, A. (2001) *Faseb J* **15**, 341-350
25. Congote, L. F., and Temmel, N. (2004) *FEBS Lett* **576**, 343-347
26. Roberts, D. D., Cashel, J., and Guo, N. (1994) *J Tissue Cult Methods* **16**, 217-222
27. Misenheimer, T. M., and Mosher, D. F. (2005) *J Biol Chem* **280**, 41229-41235
28. Annis, D. S., Gunderson, K. A., and Mosher, D. F. (2007) *J Biol Chem* **282**, 27067-27075
29. Piccio, L., Vermi, W., Boles, K. S., Fuchs, A., Strader, C. A., Facchetti, F., Cella, M., and Colonna, M. (2005) *Blood* **105**, 2421-2427
30. Guo, N. H., Krutzsch, H. C., Negre, E., Vogel, T., Blake, D. A., and Roberts, D. D. (1992) *Proc Natl Acad Sci U S A* **89**, 3040-3044
31. Chandrasekaran, S., Guo, N. H., Rodrigues, R. G., Kaiser, J., and Roberts, D. D. (1999) *J Biol Chem* **274**, 11408-11416
32. Li, Z., Calzada, M. J., Sipes, J. M., Cashel, J. A., Krutzsch, H. C., Annis, D. S., Mosher, D. F., and Roberts, D. D. (2002) *J Cell Biol* **157**, 509-519
33. Calzada, M. J., Annis, D. S., Zeng, B., Marcinkiewicz, C., Banas, B., Lawler, J., Mosher, D. F., and Roberts, D. D. (2004) *J Biol Chem* **279**, 41734-41743
34. Brown, E. J., and Frazier, W. A. (2001) *Trends Cell Biol* **11**, 130-135
35. Munson, P. J., and Rodbard, D. (1980) *Anal Biochem* **107**, 220-239
36. Subramanian, S., Parthasarathy, R., Sen, S., Boder, E. T., and Discher, D. E. (2006) *Blood* **107**, 2548-2556
37. Maile, L. A., and Clemmons, D. R. (2003) *Circ Res* **93**, 925-931
38. Isenberg, J. S., Hyodo, F., Pappan, L. K., Abu-Asab, M., Tsokos, M., Krishna, M. C., Frazier, W. A., and Roberts, D. D. (2007) *Arterioscler Thromb Vasc Biol*
39. Krady, M. M., Zeng, J., Yu, J., MacLauchlan, S., Skokos, E. A., Tian, W., Bornstein, P., Sessa, W. C., and Kyriakides, T. R. (2008) *Am J Pathol* **173**, 879-891
40. Streit, M., Riccardi, L., Velasco, P., Brown, L. F., Hawighorst, T., Bornstein, P., and Detmar, M. (1999) *Proc Natl Acad Sci U S A* **96**, 14888-14893
41. Lawler, J., and Detmar, M. (2004) *Int J Biochem Cell Biol* **36**, 1038-1045
42. Simantov, R., Febbraio, M., and Silverstein, R. L. (2005) *Matrix Biol* **24**, 27-34
43. Isenberg, J. S., Pappan, L. K., Romeo, M. J., Abu-Asab, M., Tsokos, M., Wink, D. A., Frazier, W. A., and Roberts, D. D. (2008) *Ann Surg* **247**, 180-190
44. Barazi, H. O., Li, Z., Cashel, J. A., Krutzsch, H. C., Annis, D. S., Mosher, D. F., and Roberts, D. D. (2002) *J Biol Chem* **277**, 42859-42866
45. Floquet, N., Dedieu, S., Martiny, L., Dauchez, M., and Perahia, D. (2008) *Arch Biochem Biophys* **478**, 103-109
46. Rebres, R. A., Vaz, L. E., Green, J. M., and Brown, E. J. (2001) *J Biol Chem* **276**, 34607-34616
47. Isenberg, J. S., Maxhimer, J. B., Hyodo, F., Pendrak, M. L., Ridnour, L. A., DeGraff, W. G., Tsokos, M., Wink, D. A., and Roberts, D. D. (2008) *Am J Pathol* **173**, 1100-1112
48. Kyriakides, T. R., Zhu, Y. H., Smith, L. T., Bain, S. D., Yang, Z., Lin, M. T., Danielson, K. G., Iozzo, R. V., LaMarca, M., McKinney, C. E., Ginns, E. I., and Bornstein, P. (1998) *J Cell Biol* **140**, 419-430

49. Isenberg, J. S., Hyodo, F., Pappan, L. K., Abu-Asab, M., Tsokos, M., Krishna, M. C., Frazier, W. A., and Roberts, D. D. (2007) *Arterioscler Thromb Vasc Biol* **27**, 2582-2588

FIGURE LEGENDS

Fig. 1. Selective binding of the signature domain of TSP1 to CD47. ***A***, Schematic diagram of the signature domains of TSP1, TSP2 and TSP4 and other recombinant constructs used in these studies. ***B***, Wild type (WT) and JinB8 CD47 deficient ($CD47^-$) Jurkat T cells (10^6 cells/tube) were treated with the indicated concentrations of TSP1 for 15 min. then incubated with ^{125}I-E123CaG1 (0.025 μg) at room temperature on a shaker for 1 h. After centrifugation through silicone oil to remove unbound ligand, the bound radioactivity was quantified and is presented with background subtracted, * = $p<0.05$. ***C-D***, Jurkat T cells (10^6 cells/tube) were treated with CD47 antibody (B6H12) or an isotype matched control IgG1 or with peptides 7N3 and 604 (1 μM), and ^{125}I-E123CaG1 binding was quantified. ***E*,** Wild type Jurkat cells were pretreated with the indicated concentrations of E123CaG1, E123CaG2 or E1234CaG1 for 15 min., and then binding of ^{125}I-E123CaG1 was quantified.

Fig. 2. TSP1 and not TSP2 blocks SIRPα binding to CD47-bearing cells. ***A***, Inhibition of ^{125}I-SIRPα binding to CD47-expressing Jurkat cells by increasing concentrations of TSP1 (0.2-20 μg/ml) was quantified as in Fig. 1. *Inset*, Data was analyzed using Ligand software and is presented as a Scatchard plot. ***B,C***, Wild type or CD47 negative Jurkat cells (10^6 cells/well) were incubated in PBS + 0.1% BSA alone or in the presence of TSP1 (10 μg/ml) or the CD47 blocking antibody B6H12 (5 μg/ml)(**B**) or an isotype matched control IgG_1 antibody (**C**), and binding of ^{125}I-SIRPα was quantified. ***D***, ^{125}I-SIRPα (0.25 μg/ml) binding to Jurkat cells was quantified in the presence of the indicated concentrations of TSP1, E123CaG1, E123CaG2, and E1234CaG4 and is presented normalized to ^{125}I-SIRPα binding in the absence of inhibitors (± SD, n = 3).

Fig. 3. Differential effects of TSPs on NO-driven cGMP in vascular cells. ***A***, Porcine VSMC were plated at 5 x 10^5 cells/well in growth medium, weaned from serum over 48 hours, and treated in minimal medium containing 0.1% BSA with the indicated dosages of the indicated recombinant domains for 15 minutes. DEA-NO (10 μM,) was then added. After 2.5 minutes the cells were extracted, and cGMP levels were determined by immunoassay. Results are presented as the mean of duplicate determinations normalized to NO-stimulated cGMP levels in VSMC and are representative of three or more independent experiments. ***B***, ***C, D,*** Porcine VSMC were treated as in *A* using the indicated proteins before assessing NO-stimulated cGMP levels except that the concentration of DEA/NO was reduced to 1 μM. E1234CaG4p = $A^{387}P$ variant of the TSP4 signature domain.

Fig. 4. NO-stimulated vascular cell adhesion to collagen is selectively inhibited by the signature domain of TSP1. ***A,B***, Human aortic VSMC were pretreated for 15 minutes with the indicated TSP recombinant domains (0.022 – 22 nM) and then plated at 10^5 cells/well in minimal medium with 0.1%BSA onto wells that were coated with collagen (3 μg/ml) in the presence (**A**) or absence (**B**) of DEA/NO (10 μM). The cells were incubated for 1 h, and adhesion was determined colorimetrically after washing the wells. ***C,*** Cells were incubated with the indicated signature domains (22 nM), and then adhesion on collagen was quantified in the presence of DEA/NO (10 μM). Results are presented as the mean ± SD of three or more experiments, * = $p<0.05$.

Fig. 5. Endogenous TSP2 does not regulate NO-stimulated responses in vascular cells. ***A***, Wild type and TSP2 null lung-derived endothelial cells were plated at 5 x 10^5 cells/well in 12-well plates in growth medium, weaned from serum over 48 hours and treated in minimal medium containing 0.1% BSA with DEA-NO (1 μM) for 2.5 min and cGMP levels were determined. Results represent the mean ± SD of three separate experiments, * = $p<0.05$. ***B***, Wild type and TSP2 null lung-derived endothelial cells were plated at 1 x 10^4 cells/well in 96-well plates in growth medium ± DETA/NO (10 μM), incubated for 72 h, and proliferation was determined using a tetrazolium salt reduction assay. ***C***, Real time PCR analysis of TSP1 and TSP2 mRNA expression in primary lung endothelial cells from wild type mice. ***D,*** Wild type

and TSP1 null lung endothelial cells were plated on 6-well plates and grown to 90% confluence in standard growth medium, pre-treated with a TSP2 morpholino or control (10 μM) for 48 h and then stimulated in minimal medium with 10 μM DEA/NO for 2 minutes and cGMP measured. Results represent the mean ± SD. Data from each type of vascular cells (wild type or TSP1 null) is presented normalized to basal cGMP in that cell type as 100%. ** p = 0.024 and 0.084 in two separate experiments. ***E,*** Wild type and TSP1 null endothelial cells were plated on 6-well plates, grown to 90% confluence in growth medium, treated with a TSP2 targeting morpholino or mismatch control (10 μM) for 36 h, and the conditioned medium was assayed via a heparin-capture ELISA using a murine polyclonal TSP2 antibody. Because no standard is available to quantify TSP2 concentrations, results are presented as absorbance, which is proportional to TSP1 concentration.

Fig. 6. TSP2 does not limit cutaneous tissue survival to ischemic challenge. ***A***, Wild type and TSP2 null 12 week old male mice underwent random dorsal cutaneous flaps. Flap viability was determined 72 h post-operatively. Results are presented as the mean ± SD for 5 pairs of animals. B, Laser Doppler analysis of cutaneous flap perfusion in wild type and TSP2 null flaps was performed during the first post-operative hour. Animals were maintained on 1.5% isoflurane and a core temperature of 35°C.

Fig. 7. TSP2 is not limiting for reperfusion following hindlimb arterial ligation. ***A***, Wild type and TSP2 null 12 week old male mice underwent femoral artery ligation at the inguinal ligament. Hindlimb perfusion was assessed using laser Doppler imaging during the immediate post-operative interval. Representative images are shown on the left, and integrated Doppler signals from 5 pairs of animals are presented as the mean ± SD on the right panel. ***B***, The mice were reanalyzed 72 h post-operatively.

Fig 1

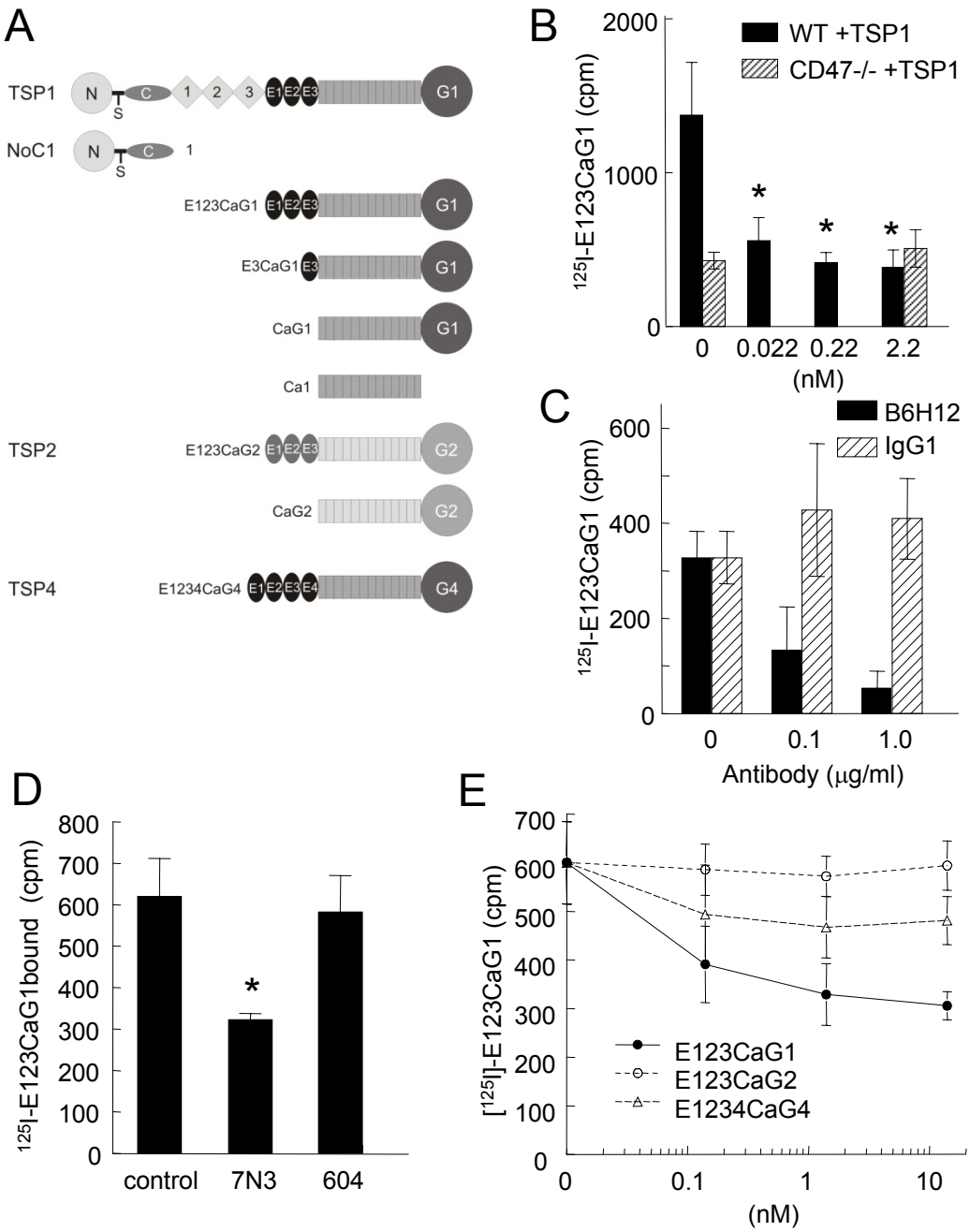
A
TSP1
N
C
S
1
2
3
E1
E2
E3
G1
NoC1
E123CaG1
E3CaG1
CaG1
Ca1
TSP2
E123CaG2
G2
CaG2
TSP4
E1234CaG4
E4
G4
B
WT +TSP1
CD47-/- +TSP1
125I-E123CaG1 (cpm)
2000
1000
0
0
0.022
0.22
2.2
(nM)
C
B6H12
IgG1
125I-E123CaG1 (cpm)
600
400
200
0
0
0.1
1.0
Antibody (μg/ml)
D
125I-E123CaG1bound (cpm)
800
700
600
500
400
300
200
100
0
control
7N3
604
E
[125I]-E123CaG1 (cpm)
700
600
500
400
300
200
100
0
E123CaG1
E123CaG2
E1234CaG4
0
0.1
1
10
(nM)

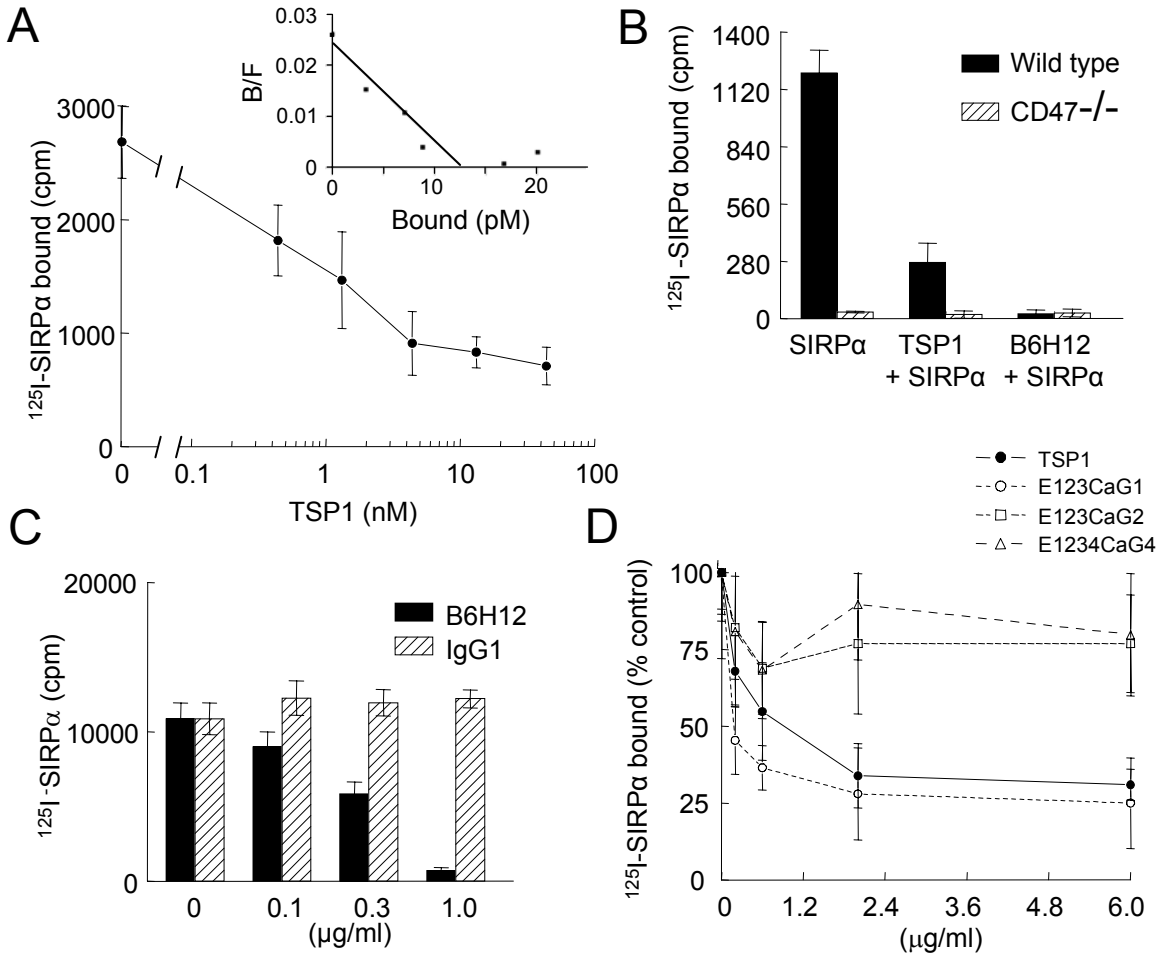
A
B/F
Bound (pM)
^{125}I-SIRPα bound (cpm)
TSP1 (nM)
B
Wild type
CD47-/-
^{125}I-SIRPα bound (cpm)
SIRPα
TSP1 + SIRPα
B6H12 + SIRPα
C
B6H12
IgG1
^{125}I-SIRPα (cpm)
(μg/ml)
D
TSP1
E123CaG1
E123CaG2
E1234CaG4
^{125}I-SIRPα bound (% control)
(μg/ml)

Fig 3

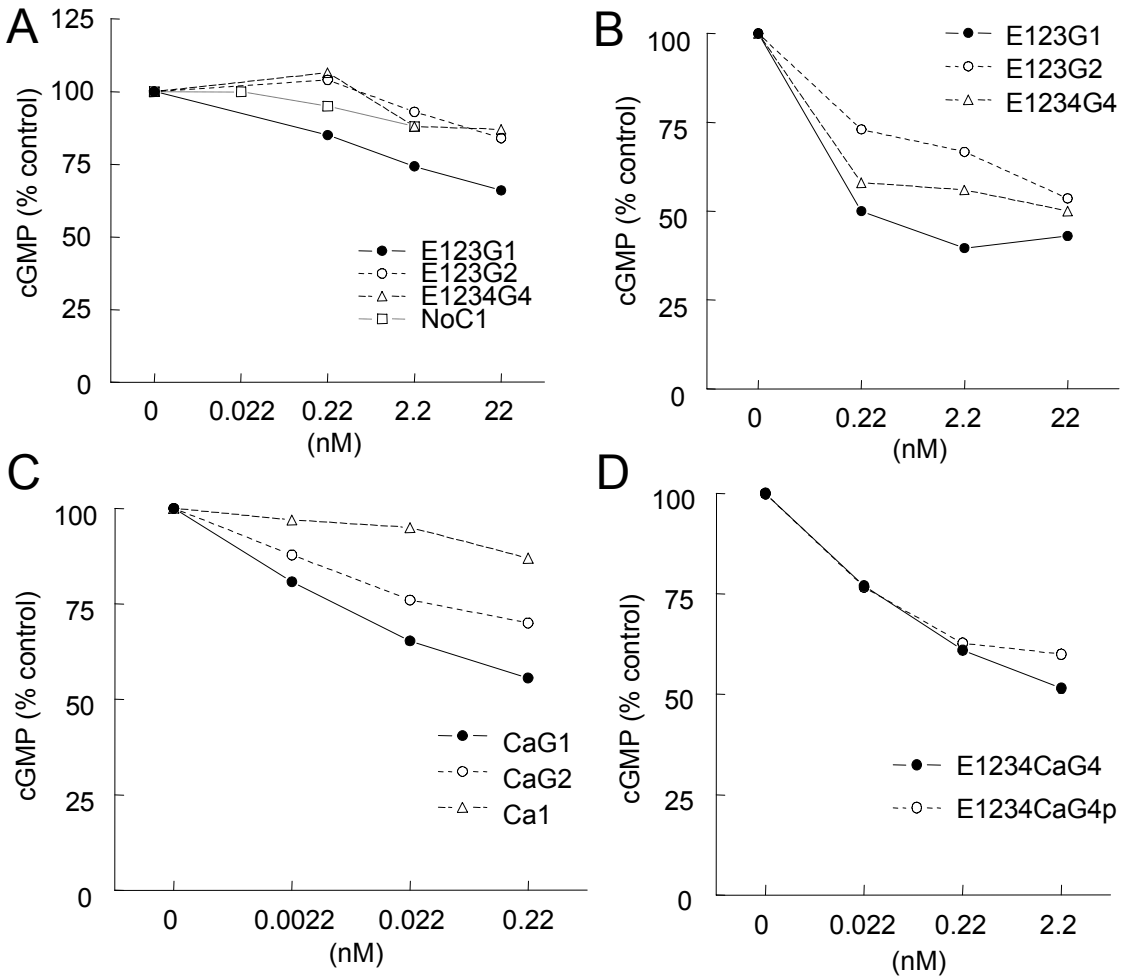
A
125
100
75
50
25
0
cGMP (% control)
E123G1
E123G2
E1234G4
NoC1
0
0.022
0.22
2.2
22
(nM)
B
100
75
50
25
0
cGMP (% control)
E123G1
E123G2
E1234G4
0
0.22
2.2
22
(nM)
C
100
75
50
25
0
cGMP (% control)
CaG1
CaG2
Ca1
0
0.0022
0.022
0.22
(nM)
D
100
75
50
25
0
cGMP (% control)
E1234CaG4
E1234CaG4p
0
0.022
0.22
2.2
(nM)

Fig 4

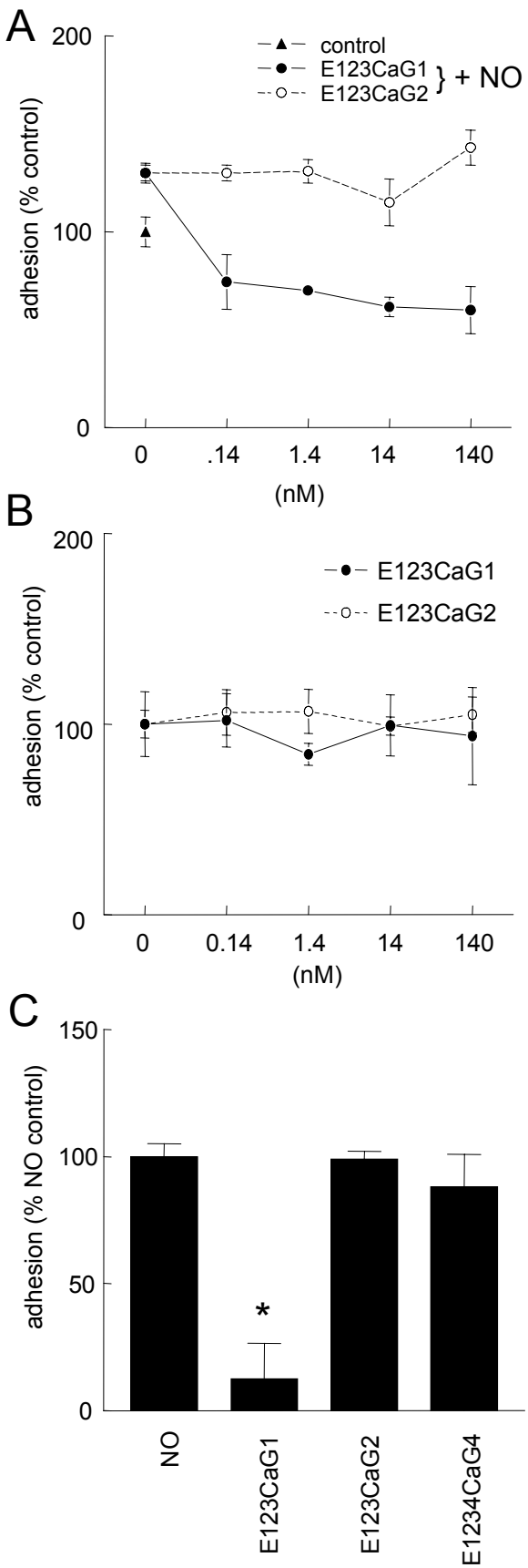
A
200
100
0
adhesion (% control)
control
E123CaG1
E123CaG2
} + NO
0
.14
1.4
14
140
(nM)
B
200
100
0
adhesion (% control)
E123CaG1
E123CaG2
0
0.14
1.4
14
140
(nM)
C
150
100
50
0
adhesion (% NO control)
*
NO
E123CaG1
E123CaG2
E1234CaG4

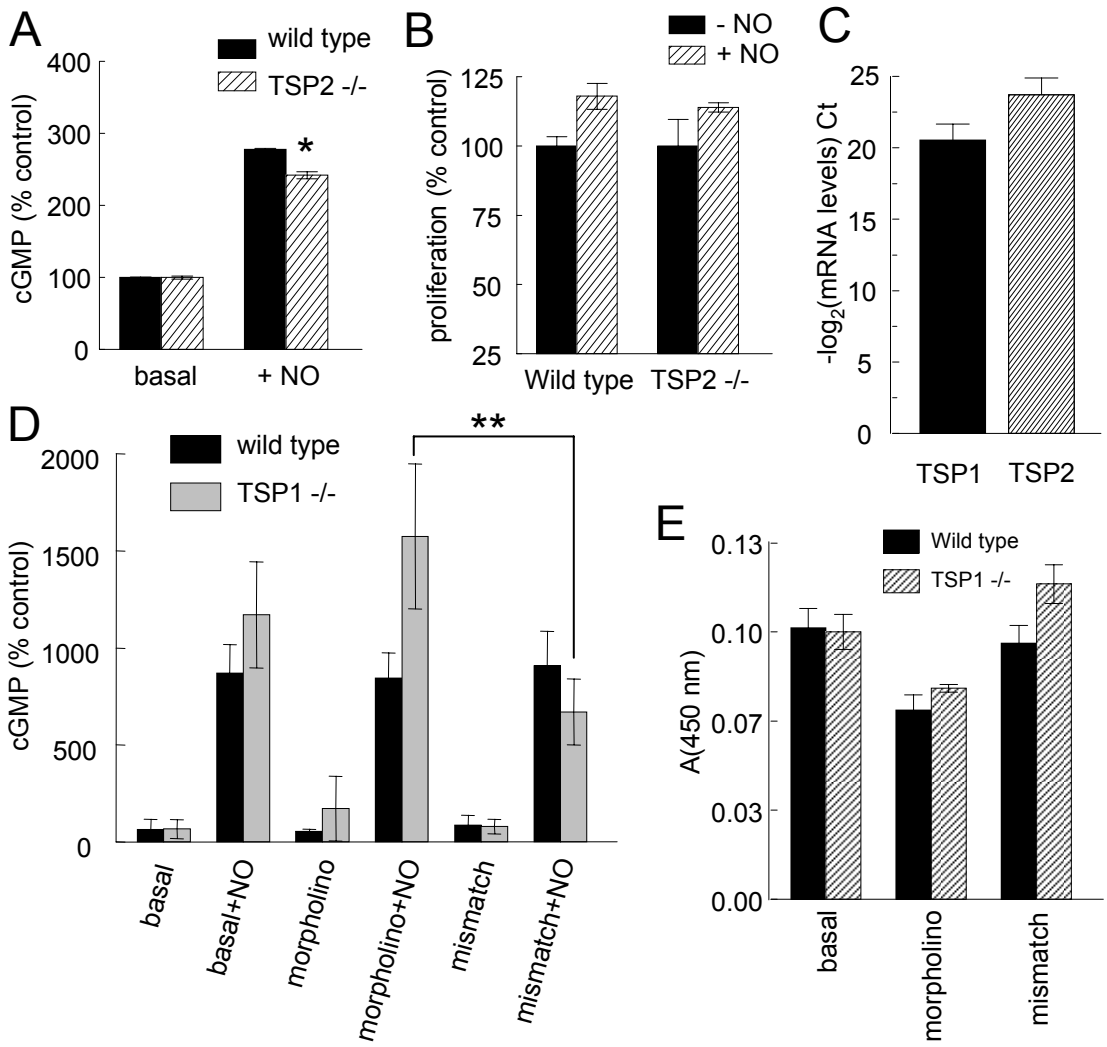
A
wild type
TSP2 -/-
cGMP (% control)
400
300
200
100
0
*
basal
+ NO
B
- NO
+ NO
proliferation (% control)
125
100
75
50
25
Wild type
TSP2 -/-
C
-log2(mRNA levels) Ct
25
20
15
10
5
0
TSP1
TSP2
D
wild type
TSP1 -/-
cGMP (% control)
2000
1500
1000
500
0
**
basal
basal+NO
morpholino
morpholino+NO
mismatch
mismatch+NO
E
Wild type
TSP1 -/-
A(450 nm)
0.13
0.10
0.07
0.03
0.00
basal
morpholino
mismatch

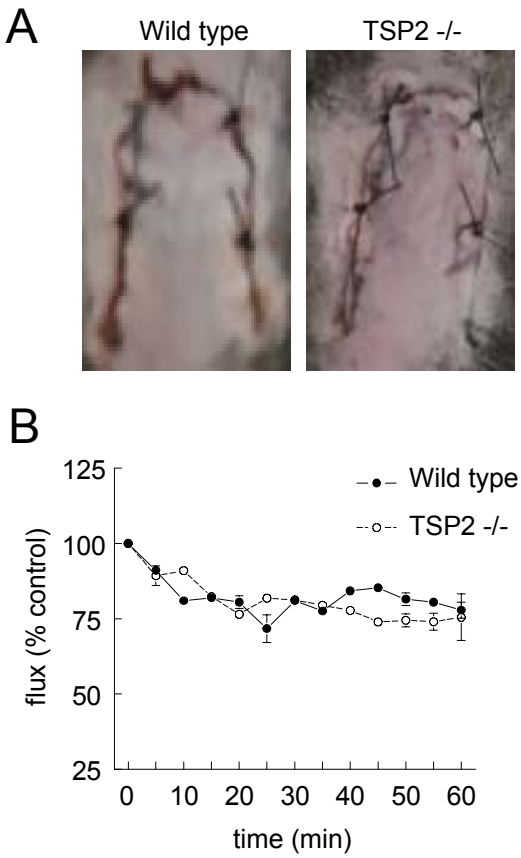
A
Wild type
TSP2 -/-
B
Wild type
TSP2 -/-
flux (% control)
125
100
75
50
25
0
10
20
30
40
50
60
time (min)

Fig. 7

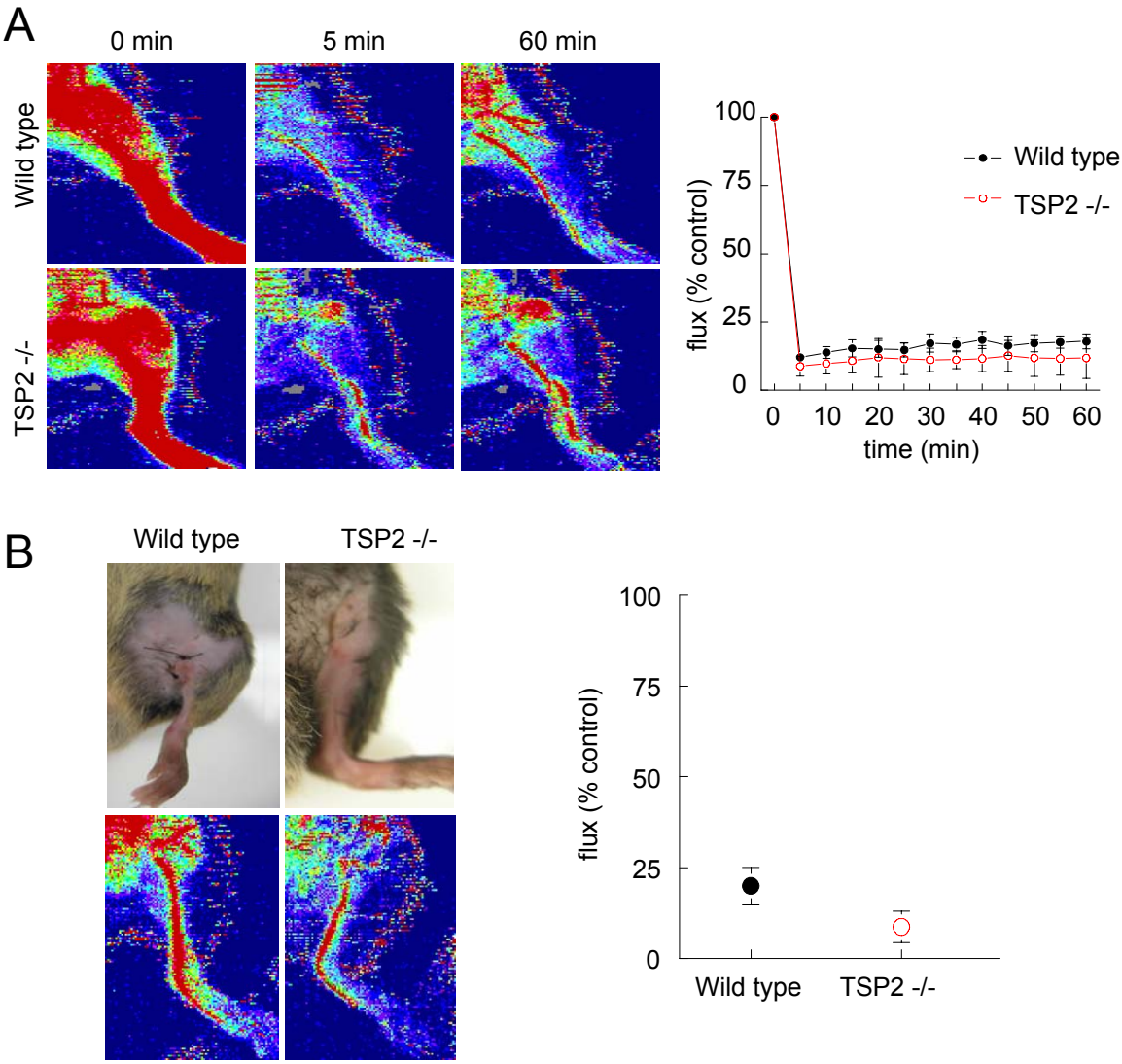
A
0 min
5 min
60 min
Wild type
TSP2 -/-
100
75
50
25
0
flux (% control)
0
10
20
30
40
50
60
time (min)
Wild type
TSP2 -/-
B
Wild type
TSP2 -/-
100
75
50
25
0
flux (% control)
Wild type
TSP2 -/-